

Supporting Information

Decoupling the Role of Carbon Counterpart in Pickering Emulsifier for Enhanced Selective Oxidation of Benzyl Alcohol

Lin Ni¹, Chang Yu^{1*}, Qianbing Wei¹, Jiangwei Chang¹, and Jieshan Qiu^{1,2*}

¹State Key Lab of Fine Chemicals, School of Chemical Engineering, Liaoning Key Lab for Energy Materials and Chemical Engineering, Dalian University of Technology, Dalian 116024, China

²College of Chemical Engineering, Beijing University of Chemical Technology, Beijing, China

**Corresponding author: E-mail: chang.yu@dlut.edu.cn (C. Yu) ;
carbon@dlut.edu.cn (J. S. Qiu)*



Scheme S1. Graphical illustration of the synthesis route for the S-1-HC-T nanocomposites.

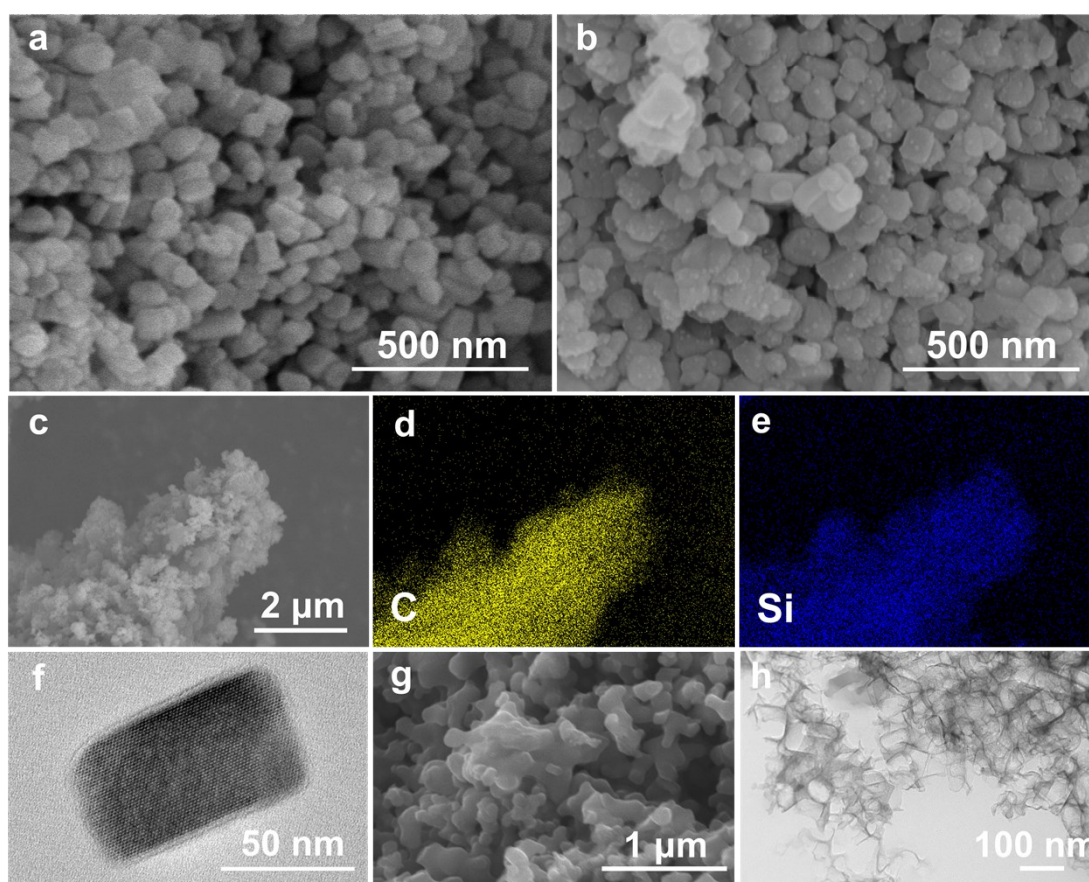


Fig. S1 The microstructure of samples. (a, b) SEM images of pristine S-1 nanoparticles and S-1-HC-700. (c) SEM image and (d, e) the corresponding C (yellow dots) and Si (blue dots) elements mapping of S-1-HC-700. (f) TEM image of S-1. (g) SEM image of HC-700. (h) TEM image of HC-700 (etched).

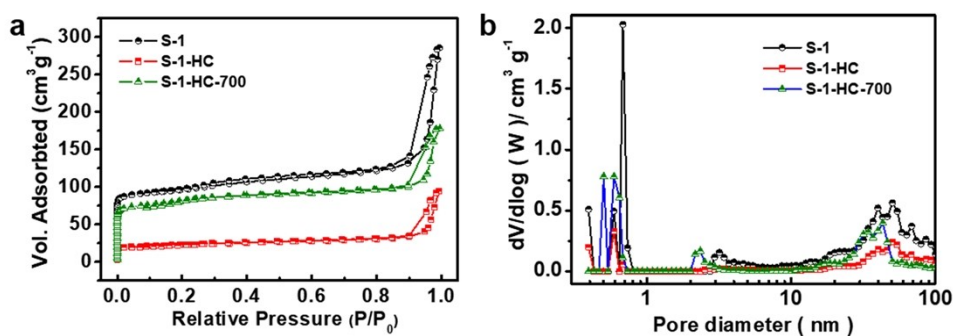


Fig. S2 (a) N_2 adsorption-desorption isotherms and (b) the corresponding pore size distributions for a series of samples.

Table S1. Chemical elemental analysis for the carbon counterparts obtained under the same hydrothermal and pyrolysis conditions without S-1 zeolite.

Samples	C (wt.%)	H (wt.%)	O (wt.%)	O/C (at.)	H/C (at.)	(O+H)/C (at.)
HC	63.32	4.68	31.65	0.375	0.887	1.262
HC-500	86.46	2.90	10.24	0.089	0.402	0.491
HC-700	93.99	1.10	4.29	0.034	0.140	0.174
HC-900	94.97	0.39	3.85	0.030	0.049	0.079

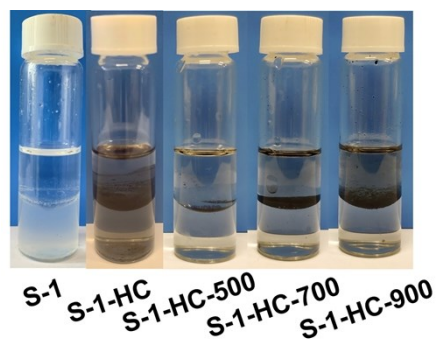


Fig. S3 Space distribution for as-obtained nanocomposites in the water/toluene biphasic system with $2.5 \text{ mg} \cdot \text{mL}^{-1}$.

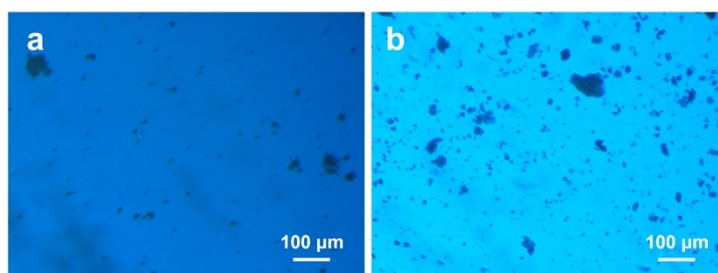


Fig. S4 Optical images of water/ toluene emulsion stabilized by (a) S-1, (b) HC.

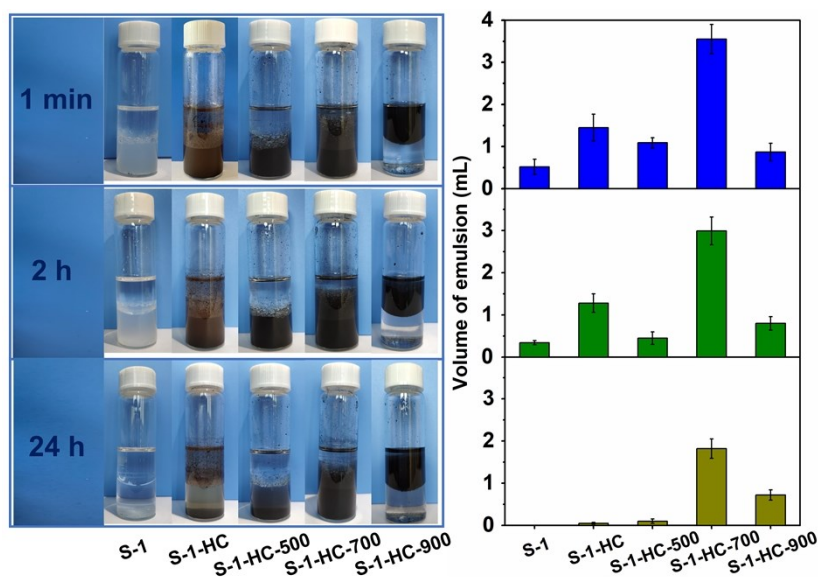
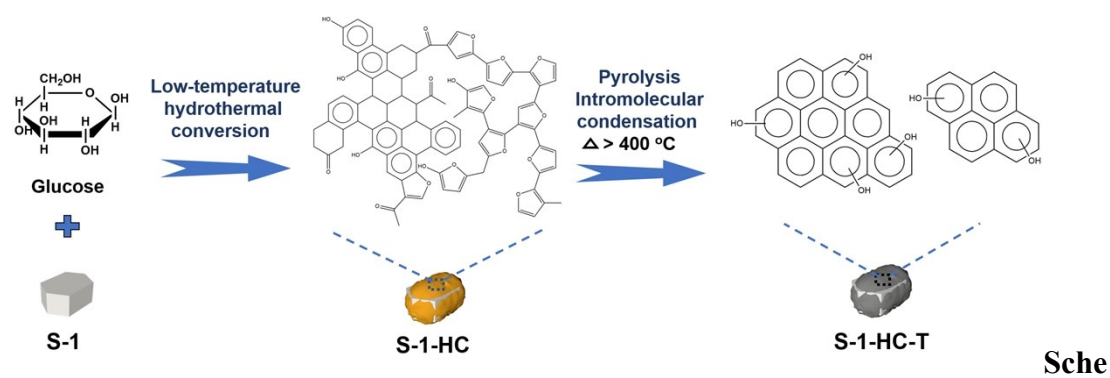


Fig. S5 Volume of Pickering emulsion stabilized by S-1 and surface modified S-1 nanocomposites, where emulsion was kept under static conditions for a different time.



me S2. Schematic illustration of the structural transformation process for glucose-derived hydrothermal carbon.

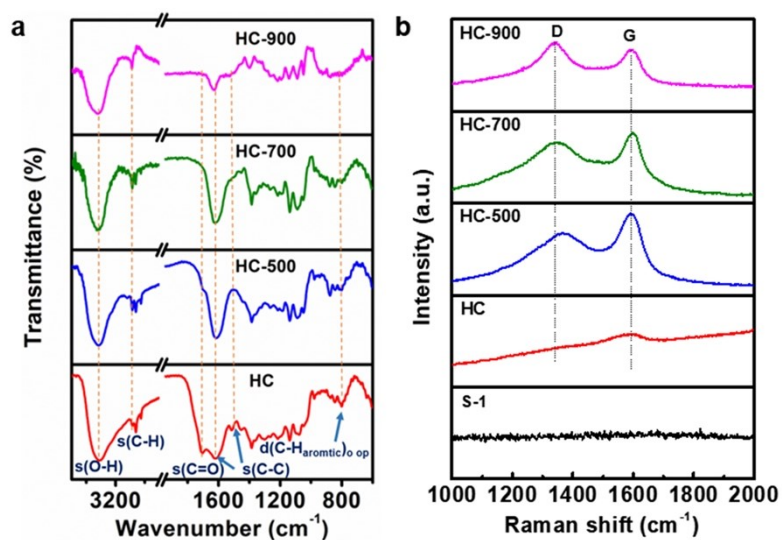


Fig. S6 Chemical structure information for a series samples. (a) FT-IR spectra of

HC and HC-T samples. (b) Raman spectra of S-1, HC, HC-500, HC-700 and HC-900.

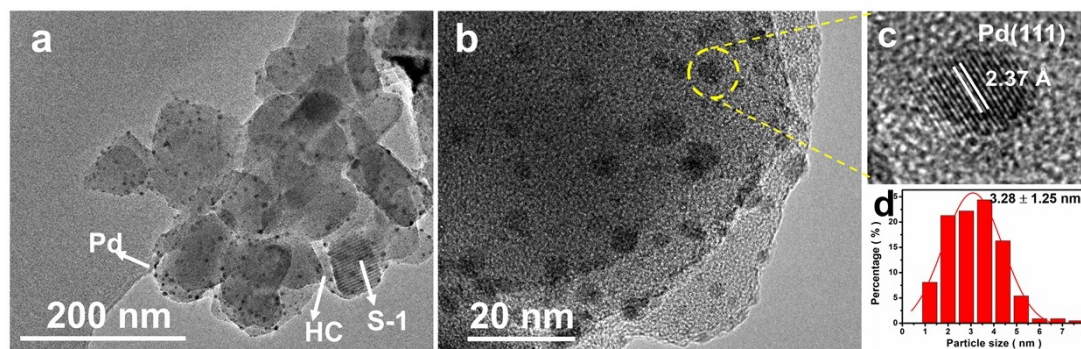


Fig. S7 (a) Low- and (b) high-magnification TEM images of Pd/S-1-HC-700. (c) High-resolution TEM image and (d) particle size distribution of the corresponding Pd nanoparticles for Pd/S-1-HC-700.

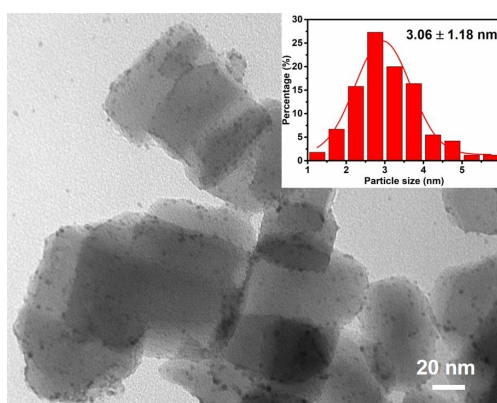


Fig. S8 TEM image of the Pd/S-1. The inset image is the particle size distribution of the corresponding Pd nanoparticles for Pd/S-1.

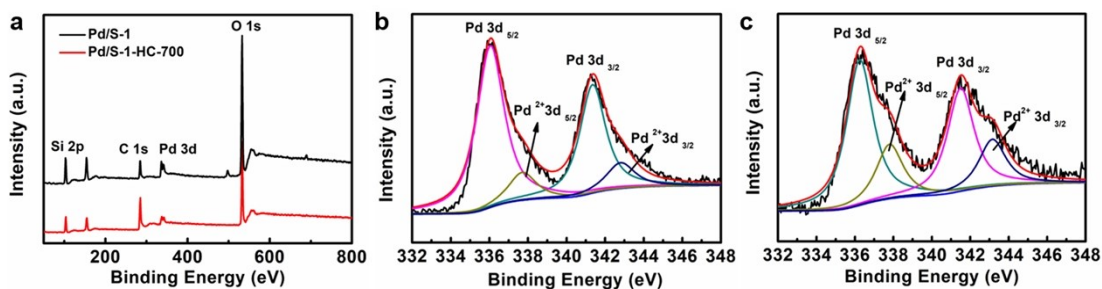
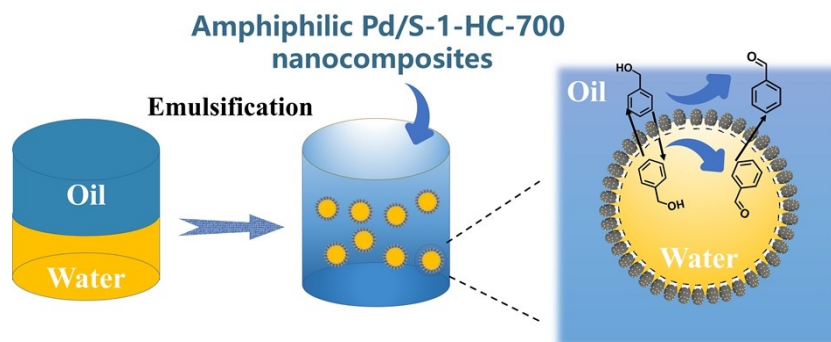


Fig. S9 (a) XPS survey spectra of Pd/S-1 and Pd/S-1-HC-700; (b) Pd 3d XPS spectra of Pd/S-1 and (c) Pd 3d XPS spectra of Pd/S-1-HC-700.

Table S2. The atomic contents of Pd (0) and Pd (2+) species for Pd/S-1 and Pd/S-1-HC-700 samples derived from XPS spectra.

Catalysts	Pd species	
	Pd (0) (at.%)	Pd (2+) (at.%)
Pd/S-1	82.90	17.10
Pd/S-1-HC-700	62.83	37.17



Scheme S3. Schematic illustration for the aerobic oxidation of benzyl alcohol catalyzed by Pd nanoparticles at the interface of oil-water with the amphiphilic Pd/S-1-HC-700.

Table S3. Catalytic performance of the different catalysts for the oxidation of benzyl alcohol.

Catalysts	Temperature (°C)	Conversion (%)	Selectivity (%)		TOF (h ⁻¹) ^[b]
			Benzaldehyde	Others ^[a]	
Pd/S-1-500	85	9.6	99.6	0.4	68.1
Pd/S-1-700	85	7.7	99.9	0.1	51.3
Pd/S-1-900	85	11.4	99.8	0.2	75.9
Pd/HC-500	85	21.6	99.9	0.1	11.0
Pd/HC-700	85	40.3	99.9	0.1	29.4
Pd/HC-900	85	25.0	99.9	0.1	9.0

[a] Benzoic acid, dibenzyl ether, and benzyl benzoate.

[b] Calculated as moles of benzyl alcohol converted per mole of total Pd per hour. A reaction time of 30 min was used. The number of active sites was calculated according to ICP test results.

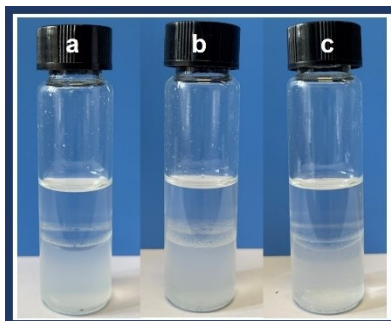


Fig. S10 Digital photos of the Pickering emulsion stabilized by (a) S-1-500, (b) S-1-700, and (c) S-1-900 in a biphasic system made of water and toluene (volume ratio: 3 mL/3 mL) after handshaking and being kept under static conditions for 1 min.

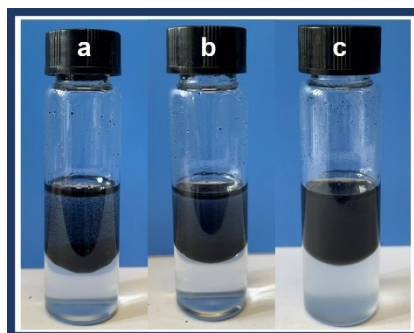


Fig. S11 Digital photos of Pickering emulsion stabilized by (a) HC-500, (b) HC-700, and (c) HC-900 in a biphasic system made of water and toluene (volume ratio: 3 mL/3 mL) after handshaking and being kept under static conditions for 1 min.

Table S4. A comparison of the Pd/S-1-HC-700 with recently reported catalysts for selective oxidation of benzyl alcohol.

Catalysts	Conversion (%)	Selectivity (%)	Temperature (°C)	Catalyst amount (mg)	Time	References
Pd/S-1-HC-700	97	99	85	50	2 h	This work
Holey HEO	98	29	120	10	2 h	Angew. Chem. Int. Ed., 2020, 59,2-9

Au ₃₈ /LDH	63	99	100	-	10 min	J. Catal., 2020, 389, 409-420
Pd ₁ /CeO ₂	27	100	100	10	3 h	Angew. Chem. Int. Ed., 2018, 57, 4642 -4646
4Pd/CN	33	100	80	25	3 h	Appl. Catal. A: Gen., 2017, 542, 380-388
Co-NG-750	95	97	130	5	5 h	Appl. Catal. A: Gen., 2017, 543, 61-66
Pd-P/PCF	77	85	70	10	2 h	Catal. Sci. Technol., 2018, 8, 2333-2339
Rh/RAC1	52	58	100	200	24 h	Appl. Catal. A: Gen., 2019, 570, 271-282
Pd/CNTs	98	89	90	300	6 h	Catal. Sci. Technol., 2015, 5, 4144-4153
Vac-H ₂	99	87	130	9	3 h	J. Catal., 2017, 350 21-29
Ru/CNT-TiO ₂	73	99	85	300	3 h	Chem-Eur. J. 2013, 19, 16192 -16195
Ru/LDH-CNTs	68	99	85	200	3 h	ACS Appl. Mater. Interfaces 2015, 7, 12203-12209

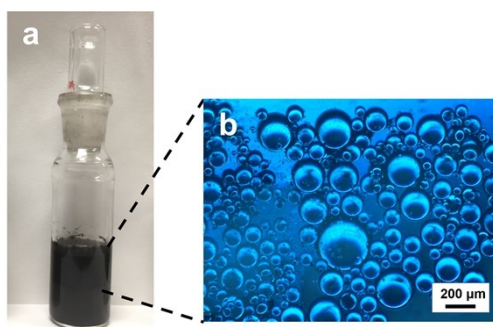


Fig. S12 Optical images of water/ toluene emulsion stabilized by Pd/S-1-HC-700 after four cycles.

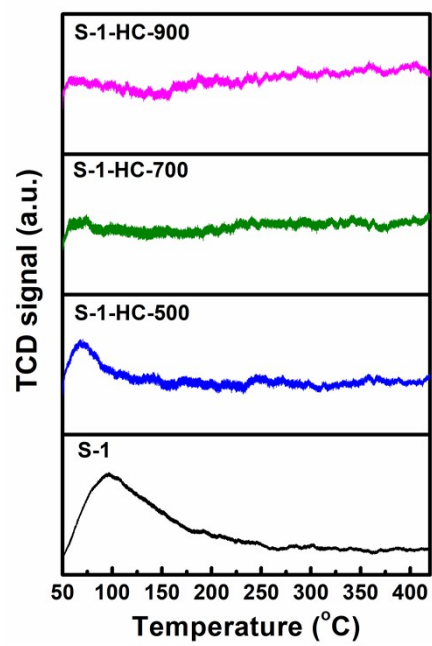


Fig. S13 CO₂-TPD profiles of S-1, S-1-HC-500, S-1-HC-700 and S-1-HC-900.